

Activated carbons from plum stones as efficient adsorbents for the removal of phenol and bisphenol A from aqueous solutions

Beata Doczekalska^{a,*}, Monika Bartkowiak^a, Krzysztof Kuśmierek^b, Andrzej Świątkowski^b

^aFaculty of Forestry and Wood Technology, Department of Chemical Wood Technology, Poznań University of Life Sciences, Poznań, Poland, emails: beata.doczekalska@up.poznan.pl (B. Doczekalska), monika.bartkowiak@up.poznan.pl (M. Bartkowiak)

^bFaculty of Advanced Technologies and Chemistry, Institute of Chemistry, Military University of Technology, Warsaw, Poland, emails: krzysztof.kusmierek@wat.edu.pl (K. Kuśmierek), a.swiatkowski@wp.pl (A. Świątkowski)

Received 17 April 2023; Accepted 3 July 2023

ABSTRACT

Activated carbons (ACs) were prepared from plum stones in a two-step process. Crushed stones were carbonized at 600°C, 700°C, or 800°C, and then chemical activation was carried out at a weight ratio of 1:4 (carbonizate to KOH), at 150°C higher than the carbonization temperature. The parameters of the porous structure and the content of surface oxygen groups were determined. The plum stone-derived activated carbons were tested as adsorbents for the removal of phenol (Ph) and bisphenol A (BPA) from aqueous solutions. The adsorption kinetics, adsorption isotherms as well as the effect of solution pH were investigated. It was observed that the adsorption was strongly pH-dependent. Adsorption was favored in the acidic pH range of 2–7 and decreased with further pH increases. The adsorption kinetics followed the pseudo-second-order model and was controlled by the film diffusion step. The Langmuir isotherm provided the best correlation for the adsorption of Ph and BPA on all of the activated carbons, and the adsorption efficiency of both the adsorbates was correlated with the specific surface area of the activated carbons. The results indicate that the ACs prepared from plum stones are efficient adsorbents for the removal of phenol and bisphenol A from aqueous solutions.

Keywords: Activated carbon; Plum stones; Adsorption; Phenol; Bisphenol A

1. Introduction

In Europe, the stone fruits are the fifth most cultivated common fruit in terms of surface area (0.6 million hectares of land) and the fourth most produced (7.3 MT). Examining the proportions of each stone fruit, peaches (*Prunus persica* L.) are the most produced, accounting for 42%, followed by plums (*Prunus domestica* L.) and nectarines (*Prunus persica* var. *nucipersica*), which account for 20% and 16% of the European production, respectively.

Finally, cherries (*Prunus avium*) and apricots (*Prunus armeniaca*) also represent an important part of stone fruit production, accounting for 13% and 9%, respectively [1].

Waste from the primary production of these fruits as well as from their processing represents a considerable potential for the production of high-quality active carbon adsorbents. The EU directives require that the disposal of such residues should be environmentally sustainable [2].

The use of agricultural by-products for activated carbon production has been noticed by many researchers [3–9]. Activated carbon fabrication is the use of various parts of plants, including the core, stems, shells, peels, flowers, fruits, seeds, leaves, husks, and also stones [10]. Among fruit stones, stones of olive [11], date [12], apricot [13], peach [14], avocado [15], cherry [16], and plum [17,18] are used as precursors of carbons.

* Corresponding author.

The literature data are the evidence illustrating that by applying different variants of fruit stone activation, it is possible to obtain a wide gamut of efficient carbon adsorbents. A very important benefit of using fruit stones as precursors is the low cost of carbon adsorbent production, following the low temperatures and short times of pyrolysis and activation. The chemical activation of such kind of biomass leads to high surface area and micro-mesoporous activated biocarbons, characterized by diverse elemental composition and acidic-basic character of the surface. Fruit stones are employed as a raw material to produce very efficient activated carbons for the treatment of polluted waters with emerging organic pollutants.

In this work, activated carbons obtained from plum stones were used as adsorbents for the removal of two common organic pollutants – phenol (Ph) and bisphenol A (BPA) from water. Phenol has found a wide range of applications in the production of phenol-formaldehyde resins, plastics, drugs, herbicides, fertilizers, dyes, detergents, or bisphenol A, which on an industrial scale is obtained by the condensation reaction of phenol with acetone in the presence of a strongly acidic ion exchange resin as a catalyst [19]. BPA itself has found application in the synthesis of polycarbonates, epoxy resins, and other polymeric materials that find general use as food and cosmetic packaging materials, among others [20,21]. The multiple and widespread uses of these compounds are the reason why they are quite common in the aquatic environment, where they can negatively affect living organisms, including humans. Both phenol and bisphenol A are toxic compounds [19–21]. The latter, due to its chemical structure similar to the estrogen 17 β -estradiol, is classified as an endocrine disrupting chemical and can act because it can act as a xenoestrogen negatively affecting the reproductive system or thyroid gland. Both compounds are suspected of having carcinogenic effects. For these reasons, the removal of both Ph and BPA from the environment is a very important matter that needs to be addressed. Among all the techniques for water purification and removal of these phenolic compounds, adsorption seems to be one of the most widely used [21–25]. Over the years, many different conventional as well as non-conventional adsorbents have been used as adsorbents [22–25]. However, there is a continuous search for new, better, less expensive adsorbents with the highest possible adsorption capacity against the mentioned pollutants. This paper, which concerns the adsorptive removal of phenol and bisphenol A from aqueous solutions on activated carbons from plum stones, fits into this trend.

2. Experimental set-up

2.1. Materials and reagents

The greengage plum stones (*Prunus domestica*) were cleaned with distilled water and dried at 105°C for 24 h. The plum stones were ground using an SM100 mill (Retsch GmbH, Haan, Germany) to a size of 0.5 mm. Biomass materials came from the Wielkopolska region (Poland).

The phenol ($\geq 99\%$) and bisphenol A ($\geq 98\%$) were received from Sigma-Aldrich (St. Louis, MO, USA). The most important properties of the two compounds as well as their structural formulas, are shown in Table 1.

2.2. Analysis of plum stones composition

Particular components of biomass (dry matter, DM) were assayed according to the TAPPI standards, including: (a) cellulose by Seifert's method using acetylacetone:dioxane mixture [26]; (b) holocellulose using sodium chlorite (TAPPI – T 9 wd-75); (c) pentosans by Tollens' method using phloroglucinol (TAPPI – T 233 cm-84); (d) lignin by the TAPPI method using concentrated sulphuric acid (TAPPI – T 222 om-06); (e) substances soluble in organic solvents according to Soxhlet (TAPPI – T 204 cm-07); and (f) ash (TAPPI – T 211 cm-86). Hemicellulose theoretical content was calculated as the difference between holocellulose and cellulose.

2.3. Preparation of activated carbons

The greengage plum stones were cleaned with distilled water and dried at 105°C for 24 h. The plum stones were ground using an SM100 mill (Retsch GmbH, Haan, Germany) and next carbonized. Pyrolysis was carried out in a chamber reactor in the oxygen-free atmosphere; the temperature increase was 3°C/min, then the final temperature (600°C, 700°C, and 800°C) was maintained for 1 h. Activation was carried out in a non-porous ceramic reactor (Czyłok, Jastrzębie-Zdrój, Poland) at a weight ratio of 1:4 (carbonizate to KOH, POCh) at 750°C, 850°C, 950°C, that is, 150°C higher than the carbonization temperature, in Ar 20 dm³/h for 30 min. Then, it was cooled in Ar 100 dm³/h, followed by extraction with 2% HCl solution (Chempur), then with deionized water to neutral pH, and finally dried at 105°C to constant weight.

The yield was defined as the final weight of the product after the processing stages of activation, washing, and drying. The percent yield was calculated from Eq. (1):

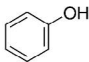
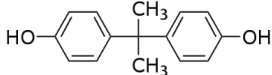
$$\text{Yield} = \frac{w_{AC}}{w_C} \times 100 [\%] \quad (1)$$

where w_{AC} – the weight of dry activated carbon (g), w_C – the weight of dry carbonizate (g).

2.4. Characterization of activated carbons

The content of CHN in samples of plum stones and carbonizates was determined using the elemental analyzer

Table 1
Physico-chemical properties of phenol and bisphenol A

Property	Phenol	Bisphenol A
CAS number	108-95-2	80-05-7
Molecular weight (g/mol)	94.11	228.29
Molecular formula	C ₆ H ₆ O	C ₁₅ H ₁₆ O ₂
Molecular structure		
Solubility in water at 25°C (g/L)	93	0.3
pKa	9.95	9.60
logP	1.48	3.41

Flash EA 2112 (Thermo Fisher Scientific, USA). The calibration of the instrument was performed with standards BBOT (2,5-bis-(tert-butyl-benzoxazol-2-yl)thiophene) and benzoic acid (Thermo Fisher Scientific, USA) and the certified reference material Alfalfa (Elemental Microanalysis Ltd., UK). For each element (C, H, N), the six-point calibration curves were plotted using the K factor as the calibration method. The correctness of the method was verified by the CHN content analysis in the certified reference material Birch leaf (Elemental Microanalysis Ltd., UK).

Thermogravimetric (TG) analysis of plum stones and carbonizates was carried out on a LabsysTM thermobalance (Setaram Instrumentation, Caluire, France) under the following conditions: final temperature 1,200°C, rate of temperature increase at 5°C/min, and helium atmosphere at the flowing rate of about 2 dm³/h. The mass loss of a sample was calculated in %.

Contents of surface oxygen groups (mmol/g) were determined according to Boehm's method [27]. Briefly, 4 samples of activated carbon, 250 mg each, were placed separately in 250 mL flasks. Then each sample was supplemented with 25 mL of 0.1 M NaOH (POCh), 0.1 M NaHCO₃ (Chempur), or 0.05 M Na₂CO₃ (POCh) (to assay acidic groups) or 0.1 M HCl (to assay basic groups), and the mixtures were shaken at ~120 rpm for 24 h at room temperature. After filtering the mixtures, 10 mL of each filtrate were pipetted, and the excess of bases and acids was titrated (Tashiro indicator) using 0.1 M HCl (POCh) or NaOH (POCh), respectively. All assays were repeated three times. Numbers of acidic sites of various types were calculated according to the formula below under the assumption that NaOH neutralizes carboxyl, phenolic and lactonic groups; Na₂CO₃ – carboxyl and lactonic ones; and NaHCO₃ only carboxyl groups. The number of surface basic sites was calculated according to the same formula, but this time from the amount of HCl which reacted with carbon.

$$G_x = (V_0 - V_x) \times c \times \frac{25}{w_x} \left[\frac{\text{mmol}}{\text{g}} \right] \quad (2)$$

where G_x – the content of functional groups of as given type; V_0 , V_x – volumes of NaOH or HCl solutions (for assays of acidic or basic groups, respectively) used for titration of assayed (V_x) and blank samples (V_0) (mL); c – HCl or NaOH concentration (mol/L); w_x – the weight of carbonizate sample (g).

The specific surface area and pore size distribution were determined by analysis of nitrogen adsorption at –196°C (ASAPTM2020, Micromeritics Instrument Corp., Norcross, GA, USA). Samples before measurement were degassed at 300°C for 10 h at a pressure of 10^{–6} Pa. Collected sorption data facilitated the calculation of the following structural parameters in the area of micro- and mesopores:

S_{BET} – specific surface area (m²/g) – by the BET method, to the relative pressure $p/p_0 \approx 0.05$ –0.2; V_t – a total pore volume (cm³/g) – determined from the isotherm at a relative pressure $p/p_0 \approx 0.975$; V_{mi} – micropore volume; V_{me} – mesopore volume.

To determine the total pore volume as well as micro- and mesopore volumes Barrett–Joyner–Halenda and t -plot methods were used.

The point of zero charge (pH_{PZC}) of activated carbons was determined by the drift method. A 20 mL each of 0.01 mol/L NaCl solution was introduced into conical flasks, the pH of which was altered by the addition of 0.1 M NaOH and/or 0.1 M HCl to obtain solutions with pH ranging from 2 to 12. Then 0.05 g of activated carbon was added to the flasks, and the mixtures were shaken for 24 h. After this time, the solutions were filtered, and their pH was measured. The final pH was plotted vs. the initial pH, and the intersection point of the resulting curve was taken as the pH_{PZC} .

2.5. Batch adsorption experiments

Adsorption studies were conducted using the batch method. 20 mL of phenol or bisphenol A solutions of appropriate concentrations and 0.01 g of weighed adsorbent (adsorbent dosage of 0.5 g/L) were introduced into conical glass flasks. The mixtures so prepared were then shaken at 22°C at a constant speed of 150 rpm. After 8 h, the solutions were filtered through filter paper and determined spectrophotometrically for Ph and/or BPA content.

The effect of solution pH on the adsorption of both adsorbates on activated carbons was investigated. The initial concentration of the adsorbates was 0.5 mmol/L. The Ph and BPA solutions, before the addition of activated carbon, were adjusted to an appropriate pH in the range of 2–11 using a small amount of 0.01 mol/L NaOH and/or HCl. After adding the adsorbents, the flasks were shaken for 8 h, and then the solutions were filtered and measured spectrophotometrically. The removal efficiency of Ph and BPA on activated carbons was evaluated using the following equation:

$$\text{Removal}[\%] = \frac{(C_0 - C_e)}{C_0} \times 100\% \quad (3)$$

where C_0 – initial concentration of Ph and/or BPA (mmol/L), C_e – concentration of adsorbate in equilibrium (mmol/L).

Studies on the effect of contact time on adsorption were carried out in a similar procedure for an initial concentration of Ph and BPA of 0.5 mmol/L. The flasks with solutions were shaken, and after a suitable time, the solutions were filtered and analyzed spectrophotometrically. This allowed the determination of the adsorption capacity after time t (q_t) according to the relationship:

$$q_t = \frac{(C_0 - C_t)V}{m} \quad (4)$$

where C_0 – initial concentration of Ph and/or BPA (mmol/L), C_t – concentration of adsorbate after time t (mmol/L), V – the volume of solution (L), m – the mass of activated carbon (g).

The study of adsorption isotherms of Ph and BPA was conducted for their solutions with initial concentrations ranging from 0.2 to 1.0 mmol/L. After 8 h, the solutions were filtered and analyzed by UV spectrophotometry. The determined adsorbate concentration after adsorption (C_e) was used to calculate the adsorption capacity (q_e) according to the following formula:

$$q_e = \frac{(C_0 - C_e)V}{m} \quad (5)$$

All batch experiments were conducted in duplicate, and the average of the two test results was used for further calculations.

A Carry 3E UV-Vis spectrophotometer (Palo Alto, CA, USA) was used to quantify Ph and BPA in solutions. Absorbance was measured at wavelengths corresponding to the absorption maxima of the adsorbates – 269 nm for Ph and 275 nm for BPA, respectively. The obtained calibration curves were linear ($R^2 \geq 0.997$) over the tested concentration range (0.05–1.0 mmol/L for Ph and 0.01–0.6 mmol/L for BPA) and were described by the following equations: $y = 1.393x + 0.017$ for Ph and $y = 2.786x + 0.047$ for BPA.

3. Results and discussion

3.1. Characterization of activated carbons

The raw plum stones used as a precursor for the preparation of activated carbons contained 26.5% cellulose, 49.3% lignin, 22.0% pentosans, 5.5% substances soluble in ethanol, and 0.58% mineral substances. The elemental analysis results for raw material and obtained carbonizates are shown in Table 2. The oxygen content was calculated from the difference.

Literature shows that each natural material requires a specific attitude because of the variety of lignocellulose materials' composition, that is, different chemical compositions and anatomic structures. The elemental composition consists of more than 40% elemental carbon (calculated per dry mass), about 50% oxygen, and up to 8% hydrogen. Among other elements, only nitrogen content exceeds 1%. The content of the major components like cellulose, hemicellulose, and lignin varies in a wide range depending on the type of material and its origin. Cellulose content usually exceeds 40% in wood, 50% in straw, and 60% in jute and hemp. Lignin content is 20%–30%, about 19%, and 14%–20%, accordingly. It is worth emphasizing that lignin content in fruit stones (plum and cherry) is about 50%, while cellulose is below 40%. Another major component of the lignocellulose materials are hemicelluloses – 15%–35% [28]. Aromatic lignin can be the source material for the production of microporous and mesoporous carbons [29], while bagasse and annual plants are for mesoporous and macroporous carbons [30,31]. High lignin content in the lignocellulose materials increases the efficiency of carbon residue since it is considered one of the most thermally stable components of biomass. Hemicelluloses decompose at 180°C–350°C, cellulose at 275°C–350°C, while lignin at 250°C–500°C [28]. Lignin is a very important component that affects the efficiency of the carbonization process [32].

Table 2
Elemental analysis results for plum stones and obtained carbonizates

	C, %	H, %	N, %	O, %	Mass loss, %
Raw material	53.32	6.63	1.38	38.67	From TG of plum stones
Carbonizates					
600°C	82.53	2.55	0.12	14.8	63.19
700°C	91.87	1.85	0.19	6.09	64.29
800°C	92.54	1.27	0.17	6.02	64.73

Surface chemistry of activated carbons obtained from carbonizates in the activation process with the use of KOH at 750°C, 850°C, and 950°C was characterized as contents of surface oxygen groups. The results are presented in Table 3.

As is revealed in Table 3, higher differences can be observed in the case of –OH groups on the surface of the activated carbons. The content of all acidic groups significantly decreases with activation temperature increase.

The porous structure parameters calculated based on determined low-temperature nitrogen adsorption isotherms (Fig. 1) are summarized in Table 4.

The porous structure of obtained activated carbons is also significantly differentiated with activation temperature. It is visible, particularly in the case of specific surface area and micropore value. The values of all porous structure parameters decrease with increasing activation temperature. Increasing the processing temperature from 750°C to 950°C resulted in a decrease in process yield (Table 4).

Table 3
Surface chemistry properties of the activated carbons from plum stones

Activated carbon	Acidic functional groups (mmol/g)				pH _{PZC}
	–COOH	–COO–	–OH	Total	
AC-750	0.15	0.15	0.74	1.04	5.65
AC-850	0.15	0.15	0.55	0.85	6.00
AC-950	0.10	0.15	0.25	0.50	6.60

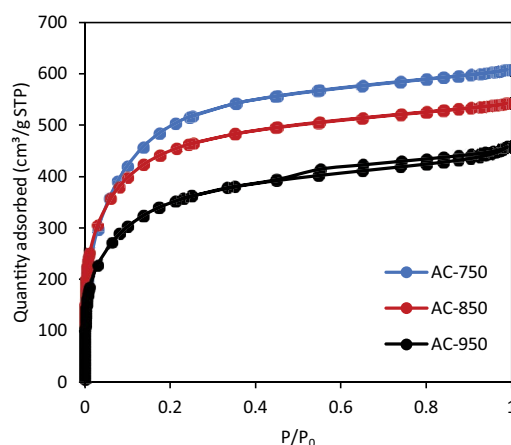


Fig. 1. Nitrogen adsorption-desorption isotherms at –196°C on plum stone-derived activated carbons.

Table 4
Yield and textural parameters of the activated carbons obtained from plum stones

Activated carbon	Yield (%)	S_{BET} (m ² /g)	V_{mi} (cm ³ /g)	V_{me} (cm ³ /g)	V_t (cm ³ /g)	V_{mi}/V_t
AC-750	60.1	1,634	0.779	0.156	0.935	83.3
AC-850	53.5	1,540	0.703	0.142	0.845	83.2
AC-950	48.4	1,177	0.555	0.134	0.689	80.6

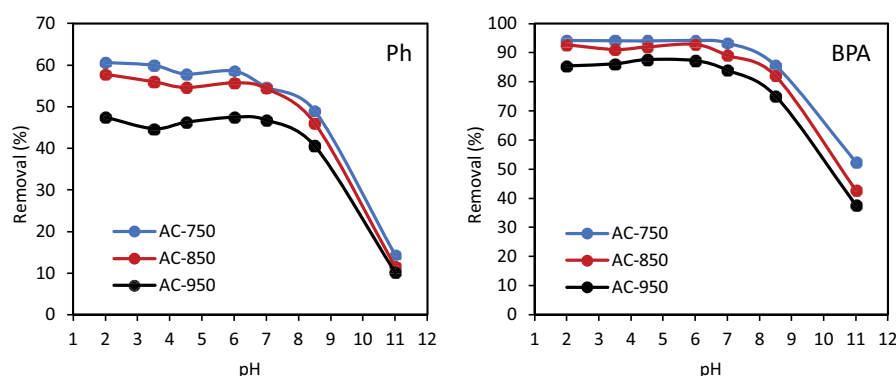


Fig. 2. Effect of pH on phenol and bisphenol A removal onto plum stone-derived activated carbons. Experimental conditions: Ph/BPA initial concentration = 0.5 mmol/L, activated carbon dosage = 0.5 g/L, temperature = 22°C.

The surface properties of the obtained activated carbons show a regularity consisting in decreasing the specific surface area and the value of other parameters of the porous structure (V_{mi} , V_{me}) and, at the same time, decreasing the amount of oxygen bound to the surface (oxygen functional groups) with the decreasing degree of activation.

For example, in the paper by Bhunthong et al. [33], one can be observed that the S_{BET} of activated carbons increased when the KOH activation temperature increased and then dropped. The decrease of S_{BET} at higher activation temperatures resulted from the continued etching of KOH on the carbon surfaces, which damaged the pore structure. The increasing further activation temperature gives widening of the existing pores and their wall breakage. When the activation temperature was increased, a decrease in yield was observed.

The degree of activation is influenced by several different factors: the type of activating agent, the temperature, and the duration of the activation process [34]. In the case of granulated activated carbons, differences in the degree of activation are also observed at different distances from the outer surface of the granule. The greater the distance from the surface (closer to the center) of the granule, the lower the degree of activation and the smaller the amount of surface oxygen functional groups when the activation is carried out for a given time and temperature of the process and the activating agent [35,36].

3.2. Adsorption study

3.2.1. Effect of solution pH

The influence of pH on phenol and bisphenol A adsorption using activated carbons from plum stone as adsorbents at pH arranging of 2–11 is illustrated in

Fig. 2. The data indicate that although BPA adsorbed more efficiently than phenol, the adsorption behavior of both adsorbates on each adsorbent was similar in the pH range studied from 2 to 11. The differences between the individual activated carbon (ACs) were not large as well. Adsorption was almost constant in the acidic pH range of 2–7 and decreased with further increases in pH (from pH 7 to 11). The percentage removal of phenol observed at pH 2 was 60.6%, 57.8%, and 47.5% for AC-750, AC-850, and AC-950, respectively, and decreased to 14.3%, 11.6%, and 10.2% in solutions at pH 11. A similar trend can be observed for BPA; when changing the pH of the solution from 2 to 11, adsorption decreased from 94.2% to 52.5% for AC-750, from 92.7% to 42.8% for AC-850, and from 85.5% to 37.7% for AC-950. A similar trend for the adsorption of both compounds with a change in solution pH was reported on various commercial activated carbons [37,38] as well as activated carbons prepared from tobacco residues [39], *Tithonia diversifolia* biomass [40], Brazil nut shell [41], rice straw [42], palm shell [43] and oil palm wastes [44].

The similar behavior of Ph and BPA on all three activated carbons, as well as the slight differences observed between individual ACs, are because both adsorbates and adsorbents have similar acid–base properties (similar values of pKa and pH_{PZC} respectively). The negative decimal logarithm of the acid's dissociation constant (pKa) determines the acid's ability to dissociate into a hydrogen ion H^+ and an anion of the acidic residue, and for weak acids such as Ph and BPA is 9.95 and 9.60, respectively (Table 1). This means that in solutions with a pH below pKa, these compounds exist in a protonated form, while in solutions with a pH > pKa, they dissociate to form phenolate and bisphenolate anions.

However, the pH of the solution determines not only the degree of ionization and speciation of the adsorbate

but also the surface charge of the adsorbent. The pH point of zero charge (pH_{PZC}) obtained for the activated carbons were 5.65, 6.00, and 6.60 for AC-750, AC-850, and AC-950, respectively. This means that at $\text{pH} < \text{pH}_{\text{PZC}}$ the surface of the activated carbon was positively charged, while at a pH higher than pH_{PZC} the surface had a net negative charge. The observed large reduction in Ph and BPA adsorption under strongly alkaline conditions (at pH above pH_{PZC} and pKa) can be attributed to electrostatic repulsion between the negatively charged adsorbent surface and the dissociated adsorbate molecules. In an acidic environment, so at $\text{pH} < \text{pKa}$ and when the adsorbent surface was positively charged, the adsorption of Ph and BPA remained maximal and almost constant, showing that the non-dissociated forms of the adsorbates are favored by the positively charged adsorbent surface. This suggests that, at least in acidic and near-natural environments, electrostatic interactions (electrostatic attraction) play a negligible role in the adsorption of these compounds on activated carbons.

Based on literature data, it is known that the adsorption of phenolic compounds on the adsorbent is the result of various specific and nonspecific interactions [22,25,45]. The most typical and important forces driving their adsorption on carbon adsorbents include π - π interactions, electrostatic attraction and repulsion, hydrophobic interactions, and hydrogen bonding interactions between phenolic compounds and adsorbent surface functional groups. And it is these types of interactions (hydrophobic and π - π interactions as well as hydrogen bonds) that are mainly responsible for the adsorption of Ph and BPA on plum stone-derived activated carbons. However, a recent study by [46] indicates a critical role in hydrophobic interactions. These authors studied BPA adsorption on activated carbon from cellulose-based cigarette butts and found that π - π interactions, electrostatic attraction, and hydrogen bonds played a marginal role in adsorption and that BPA adsorption was determined by long-range hydrophobic interaction synergized with short-range dispersion force.

3.2.2. Adsorption kinetics

Fig. 3 illustrates the effect of contact time on Ph and BPA adsorption. From the data obtained, it can be seen that

the adsorption equilibrium was established after about 2 h. To better study the adsorption kinetics, the experimental data were described by the pseudo-first-order model and the pseudo-second-order model, whose formulas can be presented as follows [47]:

$$\log(q_e - q_t) = \log q_e - \frac{k_1}{2.303} t \quad (6)$$

$$\frac{t}{q_t} = \frac{1}{k_2 q_e^2} + \frac{1}{q_e} t \quad (7)$$

where: q_e – adsorption capacity (mmol/g), q_t – adsorption capacity after time t (mmol/g), k_1 – pseudo-first-order rate constant (min^{-1}), k_2 – pseudo-second-order rate constant ($\text{g}/\text{mmol} \cdot \text{min}$).

The relevant parameters obtained here are listed in Table 5. Comparing the correlation coefficients of the two kinetic models, the highest R^2 values indicate that the pseudo-second-order model best fits the adsorption kinetics of Ph and BPA on plum stone-derived activated carbons. This is further supported by the fact that the calculated equilibrium adsorption capacities obtained for the pseudo-second-order agreed well with the experimentally determined equilibrium adsorption capacities (Table 5). The results obtained here corresponded to other investigations that the pseudo-second-order model successfully simulated the adsorption kinetics of both Ph and BPA on commercial activated carbons [37,38,48,49] as well as on activated carbons prepared from various agricultural [40,42–44] and industrial wastes [39,46,50–53].

Based on the values of the rate constants calculated for the pseudo-second-order model, it can be seen that BPA was adsorbed slightly faster than Ph. However, the k_1 values obtained for the pseudo-first-order model show an opposite relationship. Both parameters (k_1 and k_2) show in the agreement that Ph and BPA were adsorbed fastest on AC-750, followed by AC-850, and slowest on AC-950 (AC-750 > AC-850 > AC-950). This order can be explained by the porous structure of the adsorbents and, more specifically, by the volume of the mesopores of these activated carbons (Table 4). The V_{me} values for AC-750, AC-850 and AC-950

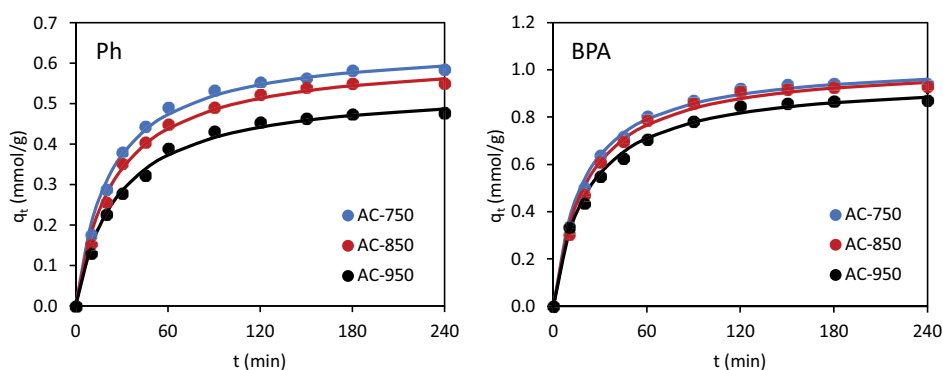


Fig. 3. Kinetic curves for phenol and bisphenol A adsorption onto plum stone-derived activated carbons (line: fitting of the pseudo-second-order kinetic model). Experimental conditions: Ph/BPA initial concentration = 0.5 mmol/L, activated carbon dosage = 0.5 g/L, pH = native (original), temperature = 22°C.

Table 5
Kinetic parameters for the adsorption of phenol and bisphenol A on activated carbon prepared from plum stones

Kinetic model/ adsorbate	Activated carbon		
	AC-750	AC-850	AC-950
Ph			
$q_{e,exp}$ (mmol/g)	0.585	0.551	0.478
Pseudo-first-order			
k_1 (min ⁻¹)	0.0295	0.0263	0.0256
$q_{e1,cal}$ (mmol/g)	0.513	0.579	0.464
R^2	0.956	0.966	0.984
Pseudo-second-order			
k_2 (g/mmol.min)	0.0695	0.0675	0.0644
$q_{e2,cal}$ (mmol/g)	0.618	0.590	0.504
R^2	0.999	0.998	0.998
BPA			
$q_{e,exp}$ (mmol/g)	0.942	0.927	0.870
Pseudo-first-order			
k_1 (min ⁻¹)	0.0361	0.0350	0.0320
$q_{e1,cal}$ (mmol/g)	1.065	1.054	0.943
R^2	0.971	0.956	0.969
Pseudo-second-order			
k_2 (g/mmol.min)	0.0522	0.0485	0.0474
$q_{e2,cal}$ (mmol/g)	1.005	0.985	0.936
R^2	0.999	0.998	0.998

were found to be 0.156, 0.142, and 0.134 cm³/g, respectively. Mesopores are very important for the rate of adsorption, as they are responsible for transporting the adsorbate to the micropores, where the surface reaction takes place. In general, the greater the mesopore volume, the faster adsorption occurs. So, in this case, it can be concluded that the adsorption rate of Ph and BPA on plum stone-derived activated carbons is correlated with their porous structure.

Although the pseudo-second-order kinetic model describes well the kinetics of Ph and BPA adsorption on the tested activated carbons, it does not give much information about the adsorption mechanism. Adsorption from solution is a multi-step process and involves: (i) external diffusion (film diffusion), that is, the transport of an adsorbate molecule from the bulk phase to the external surface of the adsorbent, (ii) intraparticle diffusion, that is the transport of adsorbate molecules from the external surface to the pores, and (iii) attachment of the adsorbate to the internal surface of the adsorbent [47]. This third and final stage is a surface reaction, which occurs very quickly and has little effect on the rate of the overall adsorption process. The rate of adsorption is determined by its slowest stage, which is the film diffusion and/or intraparticle diffusion. To determine which stage is critical for the rate of the adsorption process and also to understand the mechanism of adsorption, the Weber–Morris and Boyd kinetic models [47] were used.

The Weber–Morris model of intraparticle diffusion is described by the formula:

$$q_t = k_i t^{0.5} + C_i \quad (8)$$

where k_i – intraparticle diffusion rate constant (mmol/g·min^{-0.5}), C_i – thickness of the boundary layer.

According to the Weber–Morris diffusion model, (i) adsorption occurs only by intraparticle diffusion if the graph of $q_t = f(t^{0.5})$ is linear and passes through the origin (intercept = 0), (ii) adsorption is determined by multiple processes and not only by intraparticle diffusion if the graph of $q_t = f(t^{0.5})$ is nonlinear, and (iii) more than one process is involved in the adsorption, and the adsorption rate is determined not only by intraparticle diffusion if the graph of q_t vs. $t^{0.5}$ is nonlinear and does not pass through the origin (intercept ≠ 0).

Boyd's model is expressed by the following formulas:

$$B_t = \pi \left(1 - \sqrt{1 - \frac{\pi q_t}{3 q_e}} \right)^2 \quad \text{when } \frac{q_t}{q_e} < 0.85 \quad (9)$$

$$B_t = -0.4977 - \ln \left(1 - \frac{q_t}{q_e} \right) \quad \text{when } \frac{q_t}{q_e} > 0.85 \quad (10)$$

where B_t is a function of q_t/q_e .

According to the Boyd diffusion model, (i) the main stage that determines the adsorption is film diffusion if the graph of $B_t = f(t)$ is nonlinear (or linear) and does not pass through the origin (intercept ≠ 0), and (ii) adsorption is controlled by intraparticle diffusion only if the graph of $B_t = f(t)$ is a linear and passes through the origin (intercept = 0).

Fig. 4 shows the kinetic curves of the Weber–Morris model, while Fig. 5 presents the kinetic curves for the Boyd model. In the case of the Weber–Morris model, the curves do not pass through the point (0,0) and are multilinear, which indicates that there are multiple mechanisms controlling the adsorption process and that intraparticle diffusion does not play a primary role. The Boyd model shows that the adsorption process is determined by film diffusion since the graphs do not pass through the (0,0) point. Based on the two models used, it can be concluded that the adsorption of both adsorbates on activated carbons is a complex process influenced by both external diffusion and intraparticle diffusion and that film diffusion is the more important step determining the rate of the whole adsorption process.

3.2.3. Adsorption isotherms

Adsorption isotherms of Ph and BPA on plum stone-derived activated carbons from aqueous solutions are presented in Fig. 6. The adsorption isotherm data were fitted to the Freundlich (11) Langmuir (12), and Temkin (13) models, the equations of which can be expressed as follows [54]:

$$q_e = K_F C_e^{1/n} \quad (11)$$

$$q_e = \frac{q_m K_L C_e}{1 + K_L C_e} \quad (12)$$

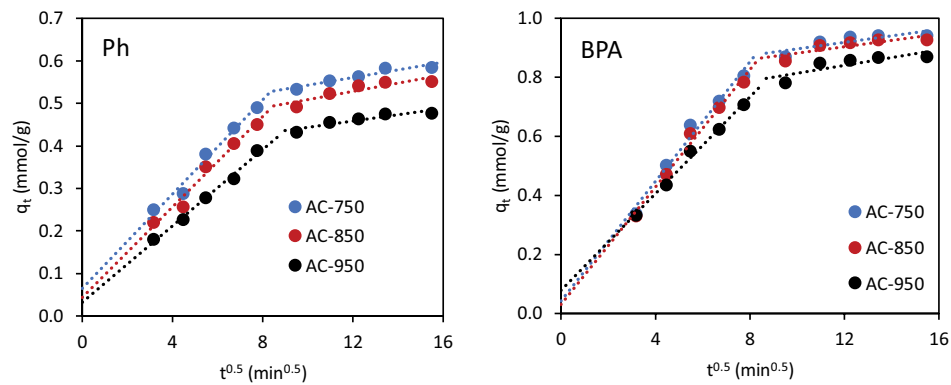


Fig. 4. Weber–Morris plot for phenol and bisphenol A adsorption onto activated carbons obtained from plum stones.

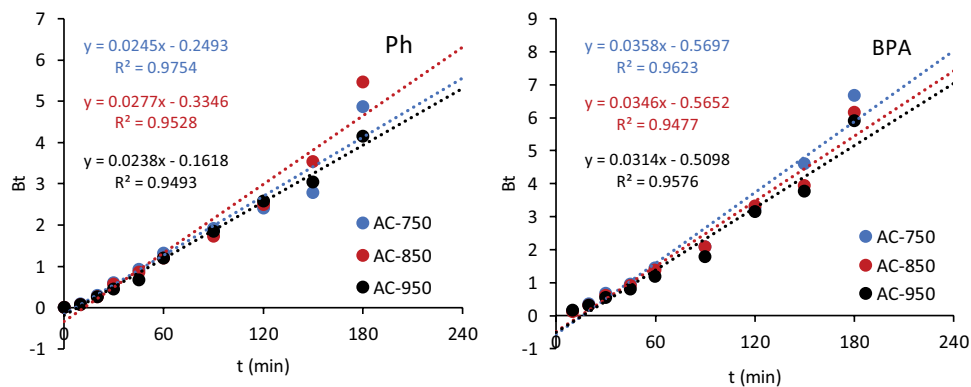


Fig. 5. Boyd plot for phenol and bisphenol A adsorption onto plum stone-derived activated carbons.

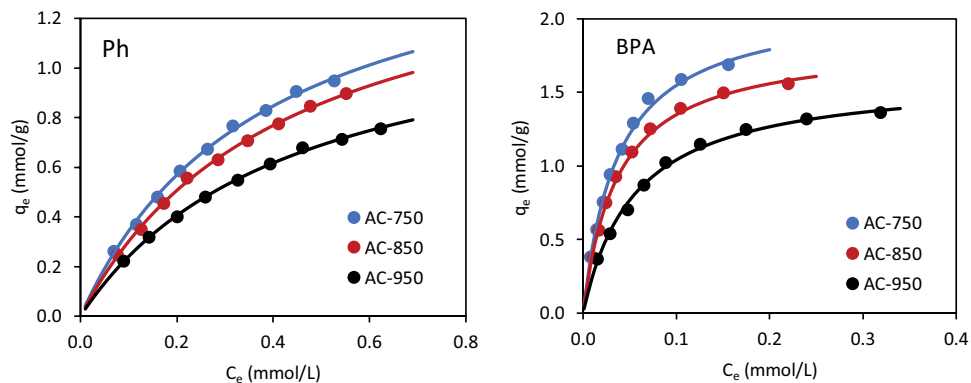


Fig. 6. Adsorption isotherms of phenol and bisphenol A onto plum stone-derived activated carbons (line: fitting of Langmuir model). Experimental conditions: Ph/BPA initial concentrations = 0.2–1.0 mmol/L, activated carbon dosage = 0.5 g/L, pH = native (original), temperature = 22°C.

$$q_e = \frac{RT}{b_T} \ln A_T C_e \quad (13)$$

where K_F – Freundlich constant which indicates the relative adsorption capacity of the adsorbent $[(\text{mmol/g})(\text{L}/\text{mmol})^{1/n}]$, n – Freundlich isotherm constants, q_m – Langmuir maximum adsorption capacity (mmol/g), K_L – Langmuir isotherm constant (L/mmol), A_T – Temkin isotherm equilibrium binding constant (L/g), b_T – Temkin isotherm

constant (J/mol), R – universal gas constant (8.314 J/mol·K), T – temperature (K).

Adsorption isotherm parameters were calculated from the slope and intercept of the linear plots of $\ln q_e$ vs. $\ln C_e$ for Freundlich, C_e/q_e vs. C_e for Langmuir and q_e vs. $\ln C_e$ for Temkin model, respectively, and are listed in Table 6.

Analyzing the data listed in Table 6, it can be concluded that, in general, all three isotherm models used described the adsorption of Ph and BPA on activated carbons quite well. Comparing the correlation coefficients, it can be seen

Table 6

Freundlich, Langmuir, and Temkin model constants for adsorption of phenol and bisphenol A onto activated carbon prepared from plum stones

Isotherm model/adsorbate	Activated carbon		
	AC-750	AC-850	AC-950
Ph			
Freundlich			
K_f ((mmol/g)(L/mmol) ^{1/n})	1.547	1.396	1.083
1/n	0.650	0.656	0.634
R^2	0.990	0.992	0.991
Langmuir			
q_m (mmol/g)	1.658	1.592	1.293
K_L (L/mmol)	2.610	2.333	2.284
R^2	0.994	0.995	0.997
Temkin			
b_T (kJ/mol)	6.935	7.308	8.703
A_T (L/g)	26.30	23.94	22.07
R^2	0.988	0.986	0.990
BPA			
Freundlich			
K_f ((mmol/g)(L/mmol) ^{1/n})	5.319	3.766	2.629
1/n	0.518	0.460	0.442
R^2	0.953	0.926	0.950
Langmuir			
q_m (mmol/g)	2.124	1.847	1.617
K_L (L/mmol)	26.88	27.07	18.08
R^2	0.997	0.998	0.999
Temkin			
b_T (kJ/mol)	5.135	6.005	6.947
A_T (L/g)	246.5	250.2	172.2
R^2	0.986	0.978	0.980

that the model that best described the adsorption process was the Langmuir isotherm, for which the highest R^2 values were obtained. The good fit obtained with the Langmuir model suggests that the adsorption of both the adsorbates onto all of the tested ACs may involve monolayer adsorption with no interactions between adsorbate molecules as well as the homogeneous nature of the adsorbents' surface.

The Langmuir adsorption isotherm also gives some information about the nature of adsorption. The obtained K_L constants can be used to determine the separation factor (R_L) according to the relationship:

$$R_L = \frac{1}{1 + K_L C_0} \quad (14)$$

The obtained R_L values for Ph ranged from 0.227 to 0.686 and from 0.036 to 0.217 for BPA on all three activated

carbons. The R_L values less than 1 but greater than 0 indicate the favorable nature of adsorption. In other cases, when $R_L = 1$, adsorption would be linear; when ($R_L > 1$) adsorption would be unfavorable; and finally, when $R_L = 0$, adsorption would be irreversible [54]. The favorable nature of the adsorption process is also confirmed by the constant n , or rather $1/n$, of the Freundlich equation, whose value ranges from 0 to 1 (Table 6). When $1/n$ is greater than 0 but less than 1 ($0 < 1/n < 1$), then the adsorption is favorable; when $1/n = 1$, then the adsorption is irreversible, and when $1/n > 1$, then the adsorption has an unfavorable nature [54].

The values of q_m as well as K_f obtained for both adsorbates increased in the order AC-950 < AC-850 < AC-750, that is, in the order in which the specific surface area of these carbons increases. This suggests that the adsorption of Ph and BPA is correlated with the BET surface area of the activated carbons. It is known that the adsorption capacity of activated carbons depends on their textural properties such as BET surface area, micro- and mesopore volume, pore size distribution, as well as on their surface chemistry, that is, the type and number of functional groups on their surface. A higher BET surface area generally corresponds to a higher adsorption capacity, and this is the situation we are seeing in this work. Both adsorbates were adsorbed best on AC-750, that is, on activated carbon with the highest surface area (1,634 m²/g) and weakest on AC-950 with the lowest BET surface area (1,177 m²/g). As mentioned earlier, the adsorption capacity of AC is also strongly influenced by surface functional groups. Based on literature data [48,55], it is fairly well known that acidic surface functional groups do not favor the adsorption of phenolic compounds, including Ph and BPA. Acidic surface functional groups (e.g., carboxyl, lactone, and/or hydroxyl) withdraw electrons from the graphene layer and increase the affinity of activated carbons for water. This promotes the formation of a molecular cluster of water through H-bonding on the surface of the carbons, which inhibits the adsorption of the adsorbate [48,55]. Therefore, considering only the surface chemical properties of activated carbons, at least in theory, Ph and BPA should adsorb weakest on AC-750, which is the most acidic activated carbon (Table 3) and best on AC-950 carbon containing the lowest acidic surface groups. Theoretically, therefore, their adsorption capacity should increase in the order AC-750 < AC-850 < AC-950. In reality, however, this is not the case, and exactly the opposite order is observed (AC-950 < AC-850 < AC-750), which seems to be correlated with the specific surface area of these materials. This would suggest that Ph and BPA adsorption on plum seed-activated carbons is critically influenced by their textural properties rather than surface chemistry. Of course, more likely, with such large BET areas above 1,000 m²/g, the influence of the porous structure on adsorption is dominant and "covers up" any effect that would be caused by functional groups on the activated carbon surface.

As mentioned earlier, the adsorption of Ph and BPA on activated carbons is the result of various types of interactions, including H-bonding, π - π interactions, as well as hydrophobic adsorbate-adsorbent interactions. These interactions are more intense for BPA, which adsorbed better than Ph on all three activated carbons. Such variations in adsorption can probably be related to differences in

Table 7
Comparison of phenol and bisphenol A adsorption on various materials

Adsorbent	S_{BET} (m ² /g)	Adsorption capacity (mg/g)		References
		Ph	BPA	
AC-750	1,634	156.0 ^a	484.9 ^a	This study
AC-850	1,540	149.8 ^a	421.6 ^a	This study
AC-950	1,177	121.7 ^a	369.1 ^a	This study
AC from tobacco residues (ACK1)	1,634	17.8	–	[39]
AC from tobacco residues (ACK2)	1,474	45.5	–	[39]
Commercial Norit R3-ex	1,390	226.6	–	[49]
AC from oily sludge (CK2T800)	2,263	434	–	[51]
Commercial GAC950	700	–	214.1	[38]
Commercial PAC800	542	–	232.0	[38]
Commercial PAC1000	1,025	–	246.3	[38]
Commercial Sorbo-Norit, 3-A-7472	1,225	–	129.6	[37]
Commercial Merck, K27350518015	1,084	–	263.1	[37]
AC from almond shells	1,216	–	188.9	[37]
AC from biomass	854	–	15.69	[40]
AC from rice straw	1,305	–	181.2	[42]
Commercial WV A1100	1,777	–	375.5	[48]
Commercial F400	966	–	317.6	[48]
AC from PET waste (SK1:1)	1,060	–	253.4	[52]
AC from PET waste (SK1:5)	1,990	–	970.2	[52]
AC from palm shell	143	–	62.50	[43]
AC from empty fruit bunch of oil palm	86.6	–	41.98	[44]
AC from waste tires (AP-CO ₂)	255	–	108.0	[53]
AC from waste tires (AP-KOH)	667	–	221.0	[53]
AC from cigarette butts (AC-800)	1,838	–	839	[46]
AC from waste tires (TCP)	700	–	123.0	[50]
Graphene oxide	–	25.0	91.0	[56]
Reduced graphene oxide	–	45.0	355	[56]
Dowex L493 polymer adsorbent	1,100	78.8	308.5	[57]
Diaion SP825 polymer adsorbent	1,000	39.2	204.4	[57]
Diaion SP207 polymer adsorbent	650	25.8	156.0	[57]

^aConverted from mmol/g.

the polarity and solubility of the two compounds. In general, poorly water-soluble compounds adsorb better on the hydrophobic surface of activated carbon. A measure of a compound's hydrophobicity is the octanol-water partition coefficient ($\log P$), a higher value of which indicates a greater affinity of the adsorbate to the adsorbent surface [45]. Thus, the better adsorption of BPA than Ph on plum seed-activated carbons can be attributed to the lower solubility of BPA (0.3 vs. 93 g/L) and its higher $\log P$ value (3.41 vs. 1.48) compared to phenol. A similar trend, better adsorption of BPA than Ph, has also been reported on other adsorbents, such as graphene oxide and reduced graphene oxide [56], and various polymer adsorbents [57]. But on the other hand, there are also some reports of better Ph adsorption compared to BPA. Such a phenomenon was observed on poly (acrylonitrile-co-styrene/pyrrole) nanofibers [58] and commercially available polymeric adsorbents [59]. This suggests that the preferred adsorption of Ph or BPA is

determined by the properties of the adsorbent used in the study.

Table 7 compares the adsorption capacity of different adsorbents used for the removal of Ph and/or BPA. The Langmuir maximum adsorption capacities obtained in this study are, in most cases, larger than in most previous papers. The high Ph and BPA adsorption capacities exhibited by our activated carbons indicate that plum stones are a good precursor for the preparation of activated carbons.

4. Conclusions

Tested plum stones proved to be good feedstocks to produce activated carbons, comparable to traditional biomass sources. All obtained ACs were characterized by a rich chemical structure of the surface and a well-developed porous structure. The characterization data showed that the activation temperature of plum stones exerted a

strong effect on the AC surface chemistry as well as porosity parameters.

In this study, the adsorption of two common water contaminants, such as phenol and bisphenol A, on plum stone-derived activated carbons was investigated. It was found that the adsorption of both pollutants on all three activated carbons was strongly pH-dependent. Adsorption was favored in the pH range of 2–7 and decreased significantly with further increases in pH. Adsorption kinetic data were analyzed using pseudo-first-order, pseudo-second-order, Weber–Morris, and Boyd models. The results showed that adsorption kinetics followed the pseudo-second-order equation and that for the adsorption of both the Ph and BPA on the activated carbons, the film diffusion is a rate-determining step. The experimental equilibrium data were modeled using several isotherm models such as Freundlich, Langmuir, and Temkin. It was found that the Langmuir isotherm provided the best correlation for the adsorption of Ph and BPA on the activated carbons. The adsorption efficiency increased in the order: AC-950 < AC-850 < AC-750 and was correlated with the BET surface area of the activated carbons. The monolayer adsorption capacities were found to be 1.658, 1.592, and 1.293 mmol/g for the adsorption of Ph and 2.124, 1.847, and 1.617 mmol/g for the adsorption of BPA on AC-750, AC-850, and AC-950, respectively. The results showed that the activated carbons prepared from plum stones are very effective adsorbents for the removal of phenol and bisphenol A from water.

Acknowledgment

The authors of this paper would like to thank all those who contribute to the realization of this work. Special thanks are addressed to Mrs. Agata Pawlicka, who received activated carbons.

Funding

The research was co-financed with funds from the Department of Forestry and Wood Technology (No. 506.223.02.00).

References

- [1] M.J. Aliaño-González, J. Gabaston, V. Ortiz-Somovilla, E. Cantos-Villar, Wood waste from fruit trees: biomolecules and their applications in agri-food industry, *Biomolecules*, 12 (2022) 238, doi: 10.3390/biom12020238.
- [2] N. Voca, N. Bilandžija, V. Jurišić, A. Matin, T. Kricka, I. Sedak, Proximate, ultimate, and energy values analysis of plum biomass by-products case study: Croatia's potential, *J. Agric. Sci. Technol.*, 18 (2016) 1655–1666.
- [3] M.A. Yahya, Z. Al-Qodah, C.W. Zanariah Ngah, Agricultural bio-waste materials as potential sustainable precursors used for activated carbon production: a review, *Renewable Sustainable Energy Rev.*, 46 (2015) 218–235.
- [4] M. Danish, T. Ahmad, A review on utilization of wood biomass as a sustainable precursor for activated carbon production and application, *Renewable Sustainable Energy Rev.*, 87 (2018) 1–21.
- [5] P. Gonzalez-Garcia, Activated carbon from lignocellulosics precursors: A review of the synthesis methods, characterization techniques and applications, *Renewable Sustainable Energy Rev.*, 82 (2018) 1393–1414.
- [6] Md. S. Reza, C.S. Yun, S. Afroze, N. Radenahmad, M.S. Abu Bakar, R. Saidur, J. Taweekun, A.K. Azad, Preparation of activated carbon from biomass and its' applications in water and gas purification, A review, *Arab J. Basic Appl. Sci.*, 27 (2020) 208–238.
- [7] R. Zhu, Q. Yu, M. Li, H. Zhao, S. Jin, Y. Huang, J. Fan, J. Chen, Analysis of factors influencing pore structure development of agricultural and forestry waste-derived activated carbon for adsorption application in gas and liquid phases: a review, *J. Environ. Chem. Eng.*, 9 (2021) 105905, doi: 10.1016/j.jece.2021.105905.
- [8] J. Jjagwe, P.W. Olupot, E. Menya, H.M. Kalibbala, Synthesis and application of granular activated carbon from biomass waste materials for water treatment: a review, *J. Bioresour. Bioprod.*, 6 (2021) 292–322.
- [9] I. Neme, G. Girma Gonfa, C. Masi, Activated carbon from biomass precursors using phosphoric acid: a review, *Helion*, 8 (2022) 11940, doi: 10.1016/j.heliyon.2022.e11940.
- [10] A.A. Pelaez-Cid, M.M.M. Teutli-Leon, Lignocellulosic Precursors Used in the Synthesis of Activated Carbon - Characterization Techniques and Applications in the Wastewater Treatment. V. Hernandez-Montoya, Ed., InTechOpen, 2012.
- [11] E. Diaz, I. Sanchis, C.J. Coronella, A.F. Mohedano, Activated carbons from hydrothermal carbonization and chemical activation of olive stones: application in sulfamethoxazole adsorption, *Resources*, 11 (2022) 43, doi: 10.3390/resources11050043.
- [12] R. Sahmarani, C. Chbib, S. Net, M. Baroudi, B. Ouddane, Application of continuous column adsorption of organochlorine pesticides from contaminated water onto date stones activated carbon, *Int. J. Environ. Res.*, 15 (2021) 585–595.
- [13] H. Tizi, T. Berrama, D. Hamane, F. Ferrag-Siagh, Z. Bendjama, Characterization of new adsorbent prepared from apricot stones activated carbon mixed with amorphous SiO₂ from Algerian diatomite for removal of *p*-nitroaniline, *Acta Periodica Technologica*, 52 (2021) 73–88.
- [14] S.G. Mohammad, M.M.H. El-Sayed, Removal of imidacloprid pesticide using nanoporous activated carbons produced via pyrolysis of peach stone agricultural wastes, *Chem. Eng. Commun.*, 208 (2021) 1069–1080.
- [15] A.B. Leite, C. Saucier, E.C. Lima, G.S. dos Reis, C.S. Umpierrez, B.L. Mello, M. Shirmardi, S.L.P. Dias, C.H. Sampaio, Activated carbons from avocado seed: optimisation and application for removal of several emerging organic compounds, *Environ. Sci. Pollut. Res.*, 25 (2018) 7647–7661.
- [16] F.O. Erdogan, Characterization of the activated carbon surface of cherry stones prepared by sodium and potassium hydroxide, *Anal. Lett.*, 49 (2016) 1079–1090.
- [17] A. Pawlicka, B. Doczekalska, M. Bartkowiak, M. Janecka, Activated carbons from plum stones, *Ann. WULS – SGGW, For. Wood Technol.*, 85 (2014) 175–179.
- [18] M. Wiśniewska, M. Marciniak, M. Gęca, K. Herda, R. Pietrzak, P. Nowicki, Activated biocarbons obtained from plant biomass as adsorbents of heavy metal ions, *Materials*, 15 (2022) 5856, doi: 10.3390/ma15175856.
- [19] J. Michałowicz, W. Duda, Phenols – sources and toxicity, *Pol. J. Environ. Stud.*, 16 (2007) 347–362.
- [20] J. Michałowicz, Bisphenol A – sources, toxicity and biotransformation, *Environ. Toxicol. Pharmacol.*, 37 (2014) 738–758.
- [21] J. Xing, S. Zhang, M. Zhang, J. Hou, A critical review of presence, removal and potential impacts of endocrine disruptors bisphenol A, *Comp. Biochem. Physiol. C: Toxicol. Pharmacol.*, 254 (2022) 109275, doi: 10.1016/j.cbpc.2022.109275.
- [22] A. Dąbrowski, P. Podkościelny, Z. Hubicki, M. Barczak, Adsorption of phenolic compounds by activated carbon—a critical review, *Chemosphere*, 58 (2005) 1049–1070.
- [23] G. Liu, J. Ma, X. Li, Q. Qin, Adsorption of bisphenol A from aqueous solution onto activated carbons with different modification treatments, *J. Hazard. Mater.*, 164 (2009) 1275–1280.
- [24] A. Bhatnagar, I. Anastopoulos, Adsorptive removal of bisphenol A (BPA) from aqueous solution: a review, *Chemosphere*, 168 (2017) 885–902.

- [25] C.B. Godiya, B.J. Park, Removal of bisphenol A from wastewater by physical, chemical and biological remediation techniques. A review, *Environ. Chem. Lett.*, 20 (2022) 1801–1837.
- [26] K. Seifert, Zur Frage der Cellulose-Schnellbestimmung nach der Acetylacetone-Methode, *Das Papier*, 14 (1960) 104–106 (in German).
- [27] H.P. Boehm, Surface oxides on carbon and their analysis: a critical assessment, *Carbon*, 40 (2002) 145–149.
- [28] M.J. Antal Jr., Biomass Pyrolysis: A Review of the Literature Part 1—Carbohydrate Pyrolysis, K.W. Böer, J.A. Duffie, Eds., *Advances in Solar Energy*, Springer, Boston, MA, 1982, pp. 61–111.
- [29] M. Olivares-Marín, C. Fernández-González, A. Macías-García, V. Gómez-Serrano, Preparation of activated carbons from cherry stones by activation with potassium hydroxide, *Appl. Surf. Sci.*, 252 (2006) 5980–5983.
- [30] B. Cagnon, X. Py, A. Guillot, F. Stoeckli, G. Chambat, Contributions of hemicellulose, cellulose and lignin to the mass and the porous properties of chars and steam activated carbons from various lignocellulosic precursors, *Bioresour. Technol.*, 100 (2009) 292–298.
- [31] B. Doczekalska, M. Bartkowiak, B. Waliszewska, G. Orszulak, J. Ceraży-Waliszewska, T. Pniewski, Characterization of chemically activated carbons prepared from miscanthus and switchgrass biomass, *Materials*, 13 (2020) 1654, doi: 10.3390/ma13071654.
- [32] D.C.S. Azevedo, J.C.S. Araújo, M. Bastos-Neto, A.E.B. Torres, E.F. Jaguaribe, C.L. Cavalcante, Microporous activated carbon prepared from coconut shells using chemical activation with zinc chloride, *Microporous Mesoporous Mater.*, 100 (2007) 361–364.
- [33] S. Bhunthong, D. Aussawasathien, K. Hrimchum, S.-N. Sriphalang, Preparation and properties of activated carbon from palm shell by potassium hydroxide impregnation: effects of processing parameters, *Chiang Mai J. Sci.*, 45 (2018) 462–473.
- [34] H. Marsh, F. Rodriguez-Reinoso, *Activated Carbon*, Elsevier Science Ltd., 2006.
- [35] B. Buczek, B. Biniak, A. Świątkowski, Oxygen distribution within oxidised active carbon granules, *Fuel*, 78 (1999) 1443–1448.
- [36] A. Deryło-Marczewska, J. Goworek, A. Świątkowski, B. Buczek, Influence of differences in porous structure within granules of activated carbon on adsorption of aromatics from aqueous solutions, *Carbon*, 42 (2004) 301–306.
- [37] I. Bautista-Toledo, M.A. Ferro-García, J. Rivera-Utrilla, C. Moreno-Castilla, F.J. Vegas Fernández, Bisphenol A removal from water by activated carbon. Effects of carbon characteristics and solution chemistry, *Environ. Sci. Technol.*, 39 (2005) 6246–6250.
- [38] B. Xie, J. Qin, S. Wang, X. Li, H. Sun, W. Chen, Adsorption of phenol on commercial activated carbons: modelling and interpretation, *Int. J. Environ. Res. Public Health*, 17 (2020) 789, doi: 10.3390/ijerph17030789.
- [39] M. Kilic, E. Apaydin-Varol, A.E. Pütün, Adsorptive removal of phenol from aqueous solutions on activated carbon prepared from tobacco residues: equilibrium, kinetics and thermodynamics, *J. Hazard. Mater.*, 189 (2011) 397–403.
- [40] A. Supong, P.C. Bhomick, M. Baruah, C. Pongener, U.B. Sinha, D. Sinha, Adsorptive removal of Bisphenol A by biomass activated carbon and insights into the adsorption mechanism through density functional theory calculations, *Sustainable Chem. Pharm.*, 13 (2019) 100159, doi: 10.1016/j.scp.2019.100159.
- [41] M.C.F. da Silva, C. Schnorr, S.F. Lütke, S. Knani, V.X. Nascimento, E.C. Lima, P.S. Thue, J. Vieillard, L.F.O. Silva, G.L. Dotto, KOH activated carbons from Brazil nut shell: preparation, characterization, and their application in phenol adsorption, *Chem. Eng. Res. Des.*, 187 (2022) 387–396.
- [42] K.-L. Chang, J.-F. Hsieh, B.-M. Ou, M.-H. Chang, W.-Y. Hsieh, J.-H. Lin, P.-J. Huang, K.-F. Wong, S.-T. Chen, Adsorption studies on the removal of an endocrine-disrupting compound (Bisphenol A) using activated carbon from rice straw agricultural waste, *Sep. Sci. Technol.*, 47 (2012) 1514–1521.
- [43] H. Soni, P. Padmaja, Palm shell based activated carbon for removal of bisphenol A: an equilibrium, kinetic and thermodynamic study, *J. Porous Mater.*, 21 (2014) 275–284.
- [44] R. Wirasmita, T. Hadibarata, A.R.M. Yusoff, Z. Yusop, Removal of bisphenol A from aqueous solution by activated carbon derived from oil palm empty fruit bunch, *Water Air Soil Pollut.*, 225 (2014) 2148, doi: 10.1007/s11270-014-2148-x.
- [45] M. Sobiesiak, Chemical Structure of Phenols and Its Consequence for Sorption Processes, M. Soto-Hernandez, M. Palma-Tenango, M. del Rosario Garcia-Mateos, *Phenolic Compounds*, InTechOpen, Rijeka, Croatia, 2017.
- [46] P. Shao, J. Pei, H. Tang, S. Yu, L. Yang, H. Shi, K. Yu, K. Zhang, X. Luo, Defect-rich porous carbon with anti-interference capability for adsorption of bisphenol A via long-range hydrophobic interaction synergized with short-range dispersion force, *J. Hazard. Mater.*, 403 (2021) 123705, doi: 10.1016/j.jhazmat.2020.123705.
- [47] K.L. Tan, B.H. Hameed, Insight into the adsorption kinetics models for the removal of contaminants from aqueous solutions, *J. Taiwan Inst. Chem. Eng.*, 74 (2017) 25–48.
- [48] G. Liu, J. Ma, X. Li, Q. Qin, Adsorption of bisphenol A from aqueous solution onto activated carbons with different modification treatments, *J. Hazard. Mater.*, 164 (2009) 1275–1280.
- [49] K. Kuśmerek, A. Świątkowski, K. Skrzypczyńska, S. Błazewicz, J. Hryniewicz, The effects of the thermal treatment of activated carbon on the phenols adsorption, *Korean J. Chem. Eng.*, 34 (2017) 1081–1090.
- [50] R. Acosta, D. Nabarlantz, A. Sánchez-Sánchez, J. Jagiello, P. Gadonneix, A. Celzard, V. Fierro, Adsorption of bisphenol A on KOH-activated tyre pyrolysis char, *J. Environ. Chem. Eng.*, 6 (2018) 823–833.
- [51] N. Mojoudi, N. Mirghaffari, M. Soleimani, H. Shariatmadari, C. Belver, J. Bedia, Phenol adsorption on high microporous activated carbons prepared from oily sludge: equilibrium, kinetic and thermodynamic studies, *Sci. Rep.*, 9 (2019) 19352, doi: 10.1038/s41598-019-55794-4.
- [52] V. Gómez-Serrano, M. Adame-Pereira, M. Alexandre-Franco, C. Fernández-González, Adsorption of bisphenol A by activated carbon developed from PET waste by KOH activation, *Environ. Sci. Pollut. Res.*, 28 (2021) 24342–24354.
- [53] K. Kuśmerek, A. Świątkowski, T. Kotkowski, R. Cherbanski, E. Molga, Adsorption of bisphenol A from aqueous solutions by activated tyre pyrolysis char – effect of physical and chemical activation, *Chem. Process. Eng.*, 41 (2020) 129–141.
- [54] M.A. Al-Ghouti, D.A. Da'ana, Guidelines for the use and interpretation of adsorption isotherm models: a review, *J. Hazard. Mater.*, 393 (2020) 122383, doi: 10.1016/j.jhazmat.2020.122383.
- [55] A. Deryło-Marczewska, D. Sternik, A. Świątkowski, K. Kuśmerek, W. Gac, B. Buczek, Adsorption of phenol from aqueous and cyclohexane solutions on activated carbons with differentiated surface chemistry, *Thermochim. Acta*, 715 (2022) 179299, doi: 10.1016/j.tca.2022.179299.
- [56] X. Wang, Y. Hu, J. Min, S. Li, X. Deng, S. Yuan, X. Zuo, Adsorption characteristics of phenolic compounds on graphene oxide and reduced graphene oxide: a batch experiment combined theory calculation, *Appl. Sci.*, 8 (2018) 1950, doi: 10.3390/app8101950.
- [57] I. Ipek, N. Kabay, M. Yüksel, Separation of bisphenol A and phenol from water by polymer adsorbents: equilibrium and kinetics studies, *J. Water Process Eng.*, 16 (2017) 206–211.
- [58] M.R. El-Aassar, I.H. Alsohaimi, A.S.M. Ali, A.A. Elzain, Removal of phenol and bisphenol A by immobilized *Laccase* on poly(acrylonitrile-co-styrene/pyrrole) nanofibers, *Sep. Sci. Technol.*, 55 (2020) 2670–2678.
- [59] J. Fan, W. Yang, A. Li, Adsorption of phenol, bisphenol A and nonylphenol ethoxylates onto hyper-crosslinked and aminated adsorbents, *React. Funct. Polym.*, 71 (2011) 994–1000.